RSC Advances

PAPER

View Article Online
View Journal | View Issue

Cite this: *RSC Adv.*, 2022, **12**, 34931

Core–shell fibremats comprising a poly(AM/DAAM)/ADH nanofibre core and nylon6 shell layer are an attractive immobilization platform for constructing immobilised enzymes†

Taira Ishiguro,[a] Akiko Obata,[a] Kenji Nagata,[a] Toshihiro Kasuga[a] and Toshihisa Mizuno*[ab]

Core–shell fibremats, comprising poly(acrylamide)-*co*-poly(diacetone–acrylamide)/adipic dihydrazide [poly(AM/DAAM)/ADH] core-nanofibres and hydrophobic polymer shell layers, are a new class of platforms for constructing various immobilised enzymes. In this study, to elucidate the impacts of the shell-layer material on fibremat properties and enzymatic activities, we synthesised core–shell fibremats with shell layers comprising nylon6 or acetyl cellulose (AcCel) instead of poly(ε-caprolactone) (PCL), as in our previous study. Transmission and scanning electron microscopy images revealed that the lactase-encapsulated poly(AM/DAAM)/ADH-nylon6 and -AcCel fibremats were both constructed like the poly(AM/DAAM)/ADH-PCL one. Leakage measurements of the beforehand loaded molecules inside the core-nanofibres revealed that both fibremats exhibited efficient permeability for low-molecular-weight molecules and stable retention of enzyme molecules inside the core-nanofibres. Meanwhile, the fibremats' mechanical properties considerably depended on the choice of shell-layer material. The thermal analyses of the lactase-encapsulated fibremats revealed residual water inside the core nanofibres. The core–shell fibremats fabricated with a nylon6 or PCL shell exhibited excellent enzymatic activities (102 and 114%, respectively, compared to that of free lactase), superior to that of the same amount of free enzyme in a buffer. Furthermore, both core–shell fibremats retained over 95% of their initial enzymatic activities, even after they were re-used 10 times.

Received 20th October 2022
Accepted 29th November 2022

DOI: 10.1039/d2ra06620c

rsc.li/rsc-advances

Introduction

Enzyme immobilisation is an effective technique for applying various enzymes to industrial, cosmetic, and pharmaceutical applications such as food modification, molecular catalysts for organic synthesis, removal of grease and protein compounding dirt, sewage treatment, make-up removal, enzyme replacement therapy, gastrointestinal drugs, electrochemical sensors, *etc.*[2–7] By immobilising enzymes on substrates, the enzyme re-usability, operativity, and (sometimes) reactivity can be improved.[8–10] Therefore, several methods for immobilising enzymes have already been established,[11] and some are used in industrial applications.

Whether enzymes are immobilised 'onto a substrate' or 'into a substrate' is determined first.[12] In most cases, enzymes are immobilised 'onto a substrate' because this method improves the enzyme accessibility to substrates, which is necessary for efficient enzymatic reactions. However, proteins continuously immersed in buffers or exposed to high temperatures, organic solvents, surfactants, and proteases may be denatured. Enzymes immobilised 'into a substrate', on the other hand, should be protected from or exhibit attenuated denaturation. However, the substrate accessibility is substantially limited compared to those of enzymes immobilised 'onto a substrate'. Therefore, if good substrate accessibility can be achieved, even immobilising enzymes 'into a substrate' should enable the development of enzyme immobilisation platforms.

Electrospun fibremats are a film-type material exhibiting the characteristics of a fibre-stacked nanostructure.[13] Electrospun fibremats can be prepared using organic, inorganic, or organic/inorganic hybrid materials and a high liquid permeability is guaranteed in fibremats owing to the gaps between the constitutive nanofibres. Additionally, the large surface areas originating from the nanofibre moulding are suitable for immobilising numerous enzymes onto fibremat nanofibres, and applications have been constructed by immobilising enzymes 'onto a substrate' to date.[14] However, if enzymes are

[a]*Department of Life Science and Applied Chemistry, Graduate School of Engineering, Nagoya Institute of Technology, Gokiso-cho, Showa-ku, Nagoya, Aichi 466-8555, Japan. E-mail: toshitcm@nitech.ac.jp*

[b]*Department of Nanopharmaceutical Sciences, Graduate School of Engineering, Nagoya Institute of Technology, Gokiso-cho Showa-ku, Nagoya, Aichi 466-8555, Japan*

† Electronic supplementary information (ESI) available. See DOI: https://doi.org/10.1039/d2ra06620c

immobilised on the fibremat nanofibre surface (*i.e.*, 'onto a substrate'), they cannot be protected from undesirable conditions.

Recently, we developed techniques for immobilising and functionalising enzymes inside fibremat nanofibres (*e.g.*, 'into a substrate').[1,15–17] First, the fibremats must be insoluble in aqueous buffers. However, choosing water-insoluble hydrophobic polymers as a fibremat base material in the first step for preparing the electrospinning precursor solutions, including the hydrophobic polymer (*i.e.*, fibremat base material) and proteinous enzymes, is difficult because no suitable solvents are available for solubilising both without denaturing the proteinous enzymes. To solve this problem, we recently established the '*in situ* cross-linking during electrospinning' (SCES) method, which can be used to fabricate water-insoluble fibremats, including enzymes in nanofibres, from aqueous precursor solutions.[17] The key points of SCES are that a pair of post-cross-linkable hydrophilic polymers and corresponding bifunctional cross-linker are used and that the cross-linking between them can be promoted by vaporising the solvent. Recently, the concept of 'synthetic materials growth' [18] has attracted much attention as a technique for constructing anisotropic materials including metal clusters,[19] conjugated polymers,[20] and hydrogels[21,22] through *in situ* chemical reactions, and SCES is partly relevant to this concept. Using SCES, we prepared water-insoluble fibremats, including proteinous enzymes in the nanofibres, without denaturing the protein. To date, we have verified that SCES can be applied to poly(γ-glutamic acid)/3-(glycidyloxy)propyl trimethoxysilane[16] and poly(acrylamide)-*co*-poly(diacetone–acrylamide) [poly(AM/DAAM)]/adipic acid dihydrazide (ADH).[17] Because these network polymers solely form hydrogels in aqueous buffers,[23] the mechanical strengths were too weak to apply the fibres practically. However, wrapping the fibres with a thin layer of hydrophobic poly(ε-caprolactone) (PCL) satisfied the required mechanical strength without sacrificing the efficient enzymatic activity against low-molecular weight (Mw) substrates.[1] Such double-layered fibremats are called 'core–shell fibremats',[24] and the PCL layer is called a 'shell'. However, to date, the impacts of the shell-layer material on the enzymatic activity, operativity, and substrate re-usability have not been discussed. Therefore, in this study, we constructed enzyme-encapsulated core–shell fibremats exhibiting either acetyl cellulose (AcCel) or nylon6 shells and compared their properties. As a representative enzyme to be encapsulated in the core–shell fibremats, we chose *Aspergillus-oryzae*-derived lactase (Mw ≈ 120 kDa).[25]

Results and discussion

Construction of enzyme-encapsulated core–shell fibremats using different hydrophobic polymer shell materials

The core–shell fibremats, comprising double-layered nanofibres—exhibiting a core (called the 'core nanofibre') of poly(AM/DAAM)/ADH hydrogels, including the enzyme, and a shell (called the 'shell layer') of hydrophobic polymers such as nylon6 or AcCel—were fabricated using co-axial electrospinning. The core–shell fibremats comprising the poly(AM/DAAM)/ADH core-nanofibres and either nylon6 or AcCel shell layer were named 'poly(AM/DAAM)/ADH-nylon6' and 'poly(AM/DAAM)/ADH-AcCel', respectively. The chemical structures are shown in Fig. 1. Poly(AM/DAAM) exhibits ketone groups at the side chain of the diacetone acrylamide (DAAM) units, which can be cross-linked by forming a hydrazone bond with the two-hydrazide-group-containing cross-linker (ADH).[23] The molar ratio of the DAAM and acrylamide[26] units was set at 1 : 4, which is suitable for constructing fibremats using SCES (Fig. 2).[17]

Because the hydrazone bond formation is a bio–orthogonal reaction,[27] this cross-linking can be performed concomitantly

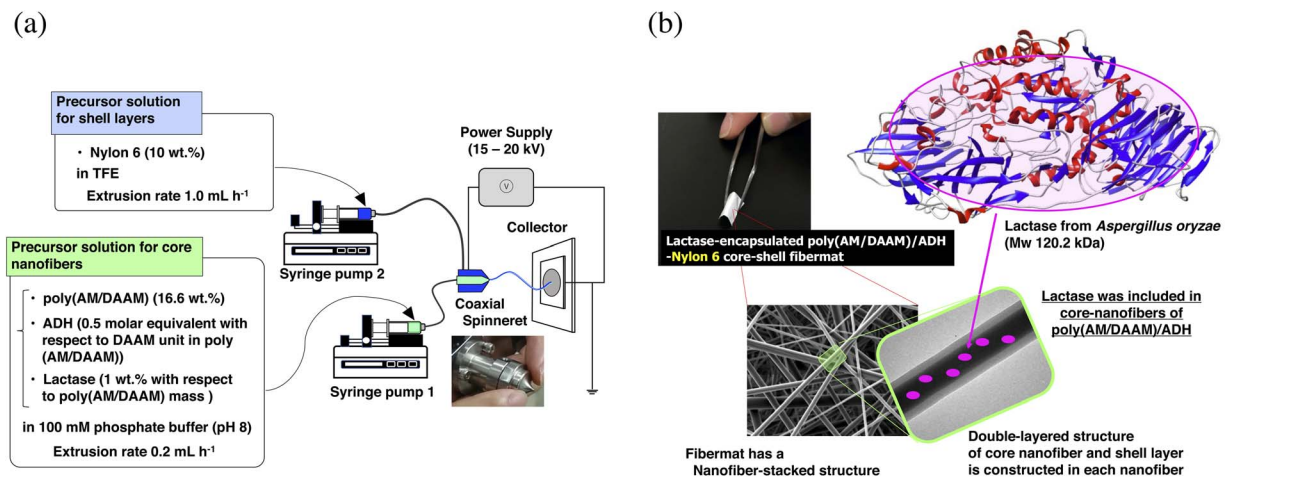

Fig. 1 (a) Schematic showing synthesis of lactase-encapsulated poly(AM/DAAM)/ADH-nylon6 core–shell fibremat by co-axial electrospinning. (b) Schematic of poly(AM/DAAM)/ADH-nylon6 core–shell fibremats encapsulating lactase in each fibremat core-nanofibre. Lactase molecules are stably held without leakage. However, low-molecular-weight (Mw) substrates can efficiently permeate in nanofibres. Therefore, encapsulated lactase can exhibit enzymatic activity for low-Mw substrate molecules solubilised in immersion buffer. Poly(AM/DAAM), poly(acrylamide)-*co*-poly(diacetone acrylamide); ADH, adipic dihydrazide; TFE, 2,2,2-trifluoroethanol; poly(AM/DAAM)/ADH, network polymers prepared by crosslinking of poly(AM/DAAM) with ADH.

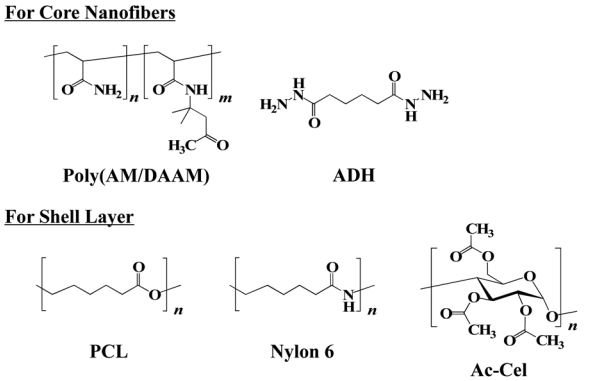

Fig. 2 Chemical structures of poly(AM/DAAM), ADH, PCL, nylon6, and acetyl cellulose (AcCel) used for constructing core–shell fibremats.

with enzyme molecules without denaturing the protein by adding ADH to the aqueous solution comprising the poly(AM/DAAM)/ADH and enzyme. Furthermore, although this reaction can progress in aqueous solutions (in the range pH 5–10), the reaction can be greatly accelerated by applying dehydration conditions. Therefore, while the solvent is vaporised (*i.e.*, dehydrated), the water-insoluble nanofibres can be electrospun *in situ*, producing water-insoluble fibremats in which the enzyme molecules are encapsulated in each nanofibre.[17] In our previous study, we called this method for constructing the protein-encapsulated fibremats the '*in situ* cross-linking during electrospinning' (SCES) method.[1,17]

Poly(AM/DAAM) was synthesised by reversible addition--fragmentation chain-transfer (RAFT) polymerisation[28] using AM and DAAM (the AM : DAAM molar ratio was set at 4 : 1), the RAFT reagent 2-(2-carboxyethylthiocarbonothioylthio) propionic acid, and the initiator VA-057, as described in a previous study.[17] The M_n and polydispersity were 46 400 and 1.55, respectively, from the gel permeation chromatography (GPC) analysis. To construct the core–shell fibremats, 20 wt% poly(AM/DAAM) dissolved in ADH-supplemented (the ADH-to-DAAM-unit molar ratio was equivalent to 0.5) 20 mM phosphate buffer (pH 8) and either 10 wt% nylon6 or 13 wt% AcCel dissolved in 2,2,2-trifluoroethanol (TFE) were extruded through a co-axial spinneret at 0.2, 1.0, or 1.2 mL h^{-1} for the core nanofibres and nylon6 or AcCel shell layers, respectively, by applying a bias of 20 kV. The morphologies of the obtained fibremats are shown in Fig. 3, and their textures were like those of the fibremats prepared using only PCL, nylon6, or AcCel.

The obtained fibremat nanostructure was examined using scanning electron microscopy (SEM) and transmission electron microscopy (TEM), as shown in Fig. 4. The SEM images of the fibremats prepared using both polymers revealed nanostructures comprising homogeneous stacked nanofibres and distinct electrospun core–shell fibremats. The TEM images also revealed the formation of the double-layered structure in each nanofibre. These findings mean that the nylon6 and AcCel can both be used to fabricate core–shell fibremats exhibiting poly(AM/DAAM)/ADH core nanofibres like the core–shell fibremats fabricated with PCL shell. As estimated from the TEM images, the average nylon6 and AcCel shell thicknesses were 23 ± 4 and 28 ± 5 nm, respectively, which were like those of the shells fabricated using PCL. Although the fibre diameters in the TEM samples appeared smaller than those in SEM ones, this can be explained by the method used to prepare TEM samples. To obtain the TEM samples of single nanofibres, we collected nanofibres at the interspace between the spinneret needle and plate collector to shorten the nanofibre collection time. Owing to different preparation procedures, although the average nanofibre diameters were different, the estimated ratio of the core diameter and shell thickness should be like those of core–shell fibremats collected on a plate collector. Using attenuated total reflection Fourier-transform infrared (ATR-FTIR) spectroscopy, we investigated the co-existence of the poly(AM/DAAM)/ADH and either nylon6 or AcCel (Fig. 4). The characteristic poly(AM/DAAM)/ADH fibremat infrared (IR) bands appeared at 1540, 1615, and 1650 cm^{-1}),[17] and additional IR bands appeared at 1034, 1204, 1393, and 1733 cm^{-1}, which are typical for the AcCel[29] in the poly(AM/DAAM)/ADH-AcCel. Owing to the intense IR bands at 1542, 1635, 2858, and 2930 cm^{-1}, which are characteristic of the nylon6 in the poly(AM/DAAM)/ADH-nylon6,[29] distinguishing both concomitant IR spectra was

Fig. 3 Series of core–shell fibremats prepared using (left; centre; right) poly(AM/DAAM)/ADH-nylon6, -AcCel, or -PCL shell, respectively.

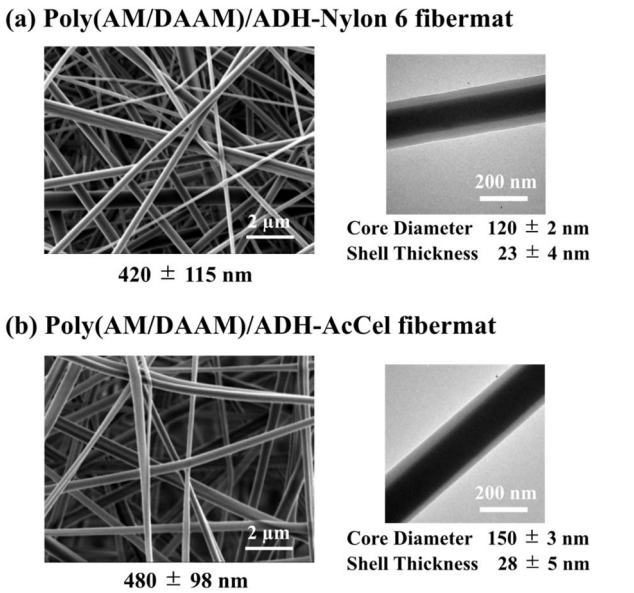

Fig. 4 SEM (left) and TEM (right) images of core–shell fibremats prepared using (a) nylon6 or (b) AcCel hydrophobic shell material. To contrast core nanofibre and shell layer, phosphotungstate salt was added to precursor solution comprising poly(AM/DAAM) and ADH before electrospinning.

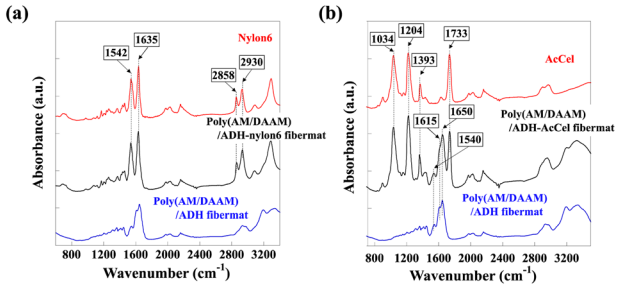

Fig. 5 AT-FTIR spectra of core–shell fibremats prepared using (a) nylon6 or (b) AcCel shell. Both spectra were compared with reference spectra for poly(AM/DAAM)ADH fibremat and nylon6 or AcCel.

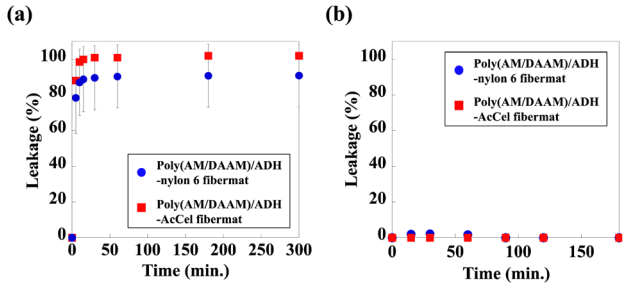

Fig. 6 Time courses for release of (a) fluorescein or (b) FITC-labelled lysozyme pre-encapsulated in core–shell fibremats prepared using either nylon6 (blue circles) or AcCel (red squares) shell layer.

difficult. However, these spectra also suggested that the core–shell fibremats were constructed with either nylon6 or AcCel shell layers (Fig. 5).

By adding lactase to the precursor solution for the core nanofibres, the lactase-encapsulated core–shell fibremats were constructed with either AcCel or nylon6 shell layers according to a similar procedure. As a reference for further experiments, lactase-encapsulated poly(AM/DAAM)/ADH-PCL was also constructed. Furthermore, because the lactase encapsulated in the core–shell fibremats must be precisely quantified for evaluating enzymatic activities, FITC-labelled lactase[30] was used in this study. *Aspergillus-oryzae*-derived lactase is a monomeric protein that exhibits a Mw of 120.2 kDa.[25] According to the SEM and TEM images, however, the lactase negligibly changed the fibremat nanostructure. The FITC-labelled lactase was extracted by solubilising the shell material and poly(AM/DAAM)/ADH core nanofibres with TFE and 1 M aqueous HCl, respectively. From the fluorescence assay, the FITC-labelled lactase contents were estimated at 2.8, 1.0, and 3.1 μg mg^{-1} [FITC-labelled lactase (μg) fibremat (mg^{-1})] in the poly(AM/DAAM)/ADH-nylon6, -PCL, and -AcCel fibremats, respectively, meaning that the encapsulation degree within core nanofibres depended on the shell material.

Molecular permeability of core–shell fibremats fabricated with nylon6 or AcCel shell layers

To perform enzymatic reactions while keeping the enzyme encapsulated in the fibremat nanofibres, not only must molecules efficiently permeate the low-Mw substrates between the outside (*i.e.*, immersion buffer) and inside of the nanofibres but also the trapped enzyme molecules must not leak from inside the nanofibres to the immersion buffer. Because the fibremat shell-layer material should considerably impact the molecular permeability, we evaluated the molecular permeability based on the leakage of pre-encapsulated low-Mw or protein molecules from the fibremat core-nanofibres to an immersion buffer before characterising the enzymatic activities. As a representative low-Mw molecule, fluorescein (Mw = 332) was chosen, as in a previous study.[1] For the encapsulating protein, we used a fluorescein isothiocyanate (FITC)-labelled lysozyme (Mw = 14.3 kDa) isolated from a hen egg white.[30] Because both molecules are fluorescent, we can estimate the leakage based on the supernatant fluorescence intensities. The core–shell fibremats were similarly constructed using the alternative core-nanofibre precursor solutions by adding 0.4 mM of fluorescein or 5 wt% of the FITC-labelled lysozyme (based on the polymer mass).

To examine the release time course, we cut a fibremat square (5 × 5 mm; 1 mg), placed in a 24-well plate and immersed in 1.0 mL of phosphate buffer for the defined time (0–300 min), and the results are shown in Fig. 6. According to Fig. 6(b), the FITC-labelled lysozyme was not released from either fibremat, meaning that the shell layer was stable regardless of the material choice and that the lysozyme remained encapsulated within the fibremat nanofibres. However, regardless of the shell-layer material [Fig. 6(a)], ~100% of the fluorescein (Mw = 332) was rapidly released within 10 min when the dried fibremat was immersed in the buffer, meaning that the poly(AM/DAAM)/ADH network structures both formed within and wrapped the nylon6 or AcCel core-nanofibres and shell layers, effectively functioning as a Mw-dependent filter, which is a suitable property for applying the core–shell fibremats to enzyme-immobilisation platforms.

In contrast to the previous expectation that the shell-material hydrophobicity considerably affected the permeability of the low-Mw hydrophilic molecule, the permeability was efficient regardless of the material possibly owing to other factors. Therefore, we used high-resolution SEM to observe the structural features (Fig. 7). During electrospinning, the solvent must be vaporised to produce the dried nanofibres. However, when several hydrophobic polymers were electrospun under highly humid conditions, pits formed in the fibremat nanofibres,[31] which is like a phenomenon called 'breath-figure self-assembly'.[32] When SCES is used to electrospin the aqueous precursor solution, the core-nanofibre solvent (*i.e.*, water)

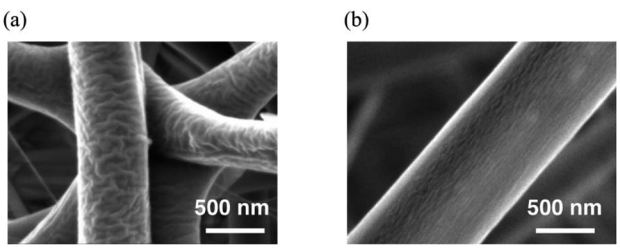

Fig. 7 High-resolution SEM images of core–shell fibremats prepared using (a) nylon6 or (b) AcCel shell layer.

should be vaporised to pass through the viscous precursor liquid flux of the shell layer. Therefore, because the hydrophobic polymers were electrospun under highly humid conditions, pits or other unique nanostructures should form, as evidenced by the unique wrinkles on the surfaces of the shell layers of both fibremats (Fig. 7). According to the findings of our previous study,[17] low-Mw molecules permeated rapidly and quantitatively though the poly(AM/DAAM)/ADH core-nanofibres. Therefore, the surface wrinkles imply that the low-Mw molecules efficiently permeated through the interconnected nanostructures regardless of the shell-layer material. Meanwhile, the previous study revealed that the FITC-labelled lysozyme molecule was large enough to be stably held in the poly(AM/DAAM)/ADH network in the core nanofibres.[1] Therefore, the core–shell fibremats can also stably hold the FITC-labelled lysozyme without any leakage.

Mechanical properties of core–shell fibremats fabricated using different hydrophobic-polymer shell materials

Our previous study revealed that un-like the PCL-shell-free poly(AM/DAAM)/ADH fibremat comprising only the nanofibres,[1] the poly(AM/DAAM)/ADH nanofibres wrapped in a thin hydrophobic PCL shell [*i.e.*, the preparation of poly(AM/DAAM)/ADH-PCL] effectively reinforced the fibremat mechanical strength (Table 1).

Therefore, we performed similar tensile tests for the core–shell fibremats and compared their mechanical properties. Each fibremat was cut into a dumbbell-shaped specimen (JIS, no. 8 dumbbell shape) and set between the sensor probes to perform the tensile tests. The obtained tensile and poly(AM/DAAM)/ADH-PCL reference data are shown in Fig. 6. The PCL sample exhibited a superior elongation at break compared to those of the nylon6 and AcCel samples. However, the nylon6 sample exhibited a superior offset yield compared to those of the other samples. Therefore, the poly(AM/DAAM)/ADH-PCL and -nylon6 exhibited a superior elongation at break and offset yield strength, respectively. Although the poly(AM/DAAM)/ADH-AcCel exhibited quite a high elastic modulus (*i.e.*, inferior elongation at break), the offset yield strength was lower than that of the poly(AM/DAAM)/ADH-nylon6, implying that the shell-layer material effectively impacted the core–shell fibremat mechanical properties (Fig. 8).

Thermal analyses of lactase-encapsulated core–shell fibremats by thermogravimetry (TG), differential thermal analysis (DTA), and differential scanning calorimetry (DSC)

To determine the amount of residual water at the core nanofibres in the core–shell fibremats, we performed thermogravimetry (TG) and differential thermal analysis (DTA) measurements for the lactase-encapsulated core–shell fibremats, freeze-dried poly(AM/DAAM)/ADH hydrogels, and FITC-labelled lactase. The TG and DTA results over the entire temperature range (30–550 °C) are presented in Fig. S1–4 (ESI),† and the data for the enlarged temperature range (30–400 °C) are shown in Fig. 9. For reference, the TG data of the freeze-dried poly(AM/DAAM)/ADH hydrogel gels (*i.e.*, core-nanofibre material) and nylon6, AcCel, and PCL powders (*i.e.*, shell-layer materials) are also presented in each graph. Below the initial temperature at which the polymer materials [such as poly(AM/DAAM)/ADH (core-nanofibre material; 230–305 °C) and nylon6, AcCel, and PCL (shell-layer materials; ~409, 330–350, and ~390 °C, respectively) thermally decomposed (<230 °C), clear weight losses corresponding to water evaporation were observed with increasing temperatures for all the fibremat samples. According to the previous TG analysis of the cross-linked polyacrylamide,[33] weight losses below 230 °C would correspond to water evaporating from the poly(AM/DAAM)/ADH polymer matrix (Fig. 9). The freeze-dried poly(AM/DAAM)/ADH hydrogels exhibited similar weight losses below 230 °C, which support this interpretation (Fig. 9). By defining the weight loss as a percentage of the fibremat weight (wt%) with increasing temperature from 30 to 200 °C as a fibremat water-content index, we evaluated the amount of residual water in the core–shell fibremats. By subtracting the weight losses (wt%) corresponding to the water adsorbed in shell materials [indicated by the black curves in Fig. 9(a)–(c)], we estimated the amount of residual water (wt%) inside the core nanofibres of the fibremats fabricated with nylon6, AcCel, or PCL shell layers at ~4.6, ~2.1, and ~2.8 wt%, respectively. The water inside the core nanofibres should contribute to the stabilisation of enzymes in the core–shell fibremats and implies that the fibremats fabricated with nylon6 shell layers were the best among all the core–shell fibremats examined to date.

We also used differential scanning calorimetry (DSC) to analyse the lactase-encapsulated core–shell fibremats, and the

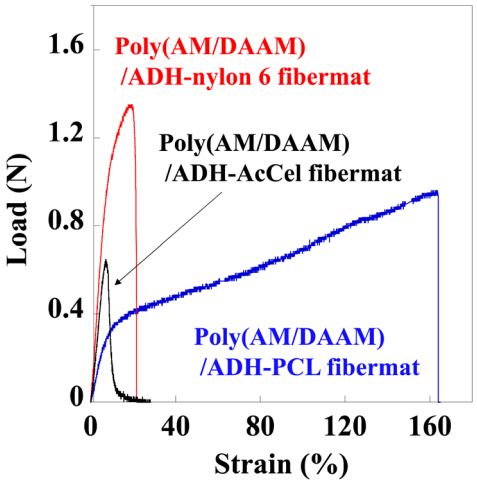

Fig. 8 Tensile test profiles of core–shell fibremats prepared using PCL, nylon6, or AcCel shell layers.

Table 1 Tensile test results of core–shell fibremats

Core–shell fibremat	Maximum load (N)	Elongation to failure (%)
Poly(AM/DAAM)/ADH-nylon6	1.18 ± 0.13	21.3 ± 3.3
Poly(AM/DAAM)/ADH-AcCel	0.68 ± 0.19	10.5 ± 2.7
Poly(AM/DAAM)/ADH-PCL	0.94 ± 0.10	163 ± 5.3

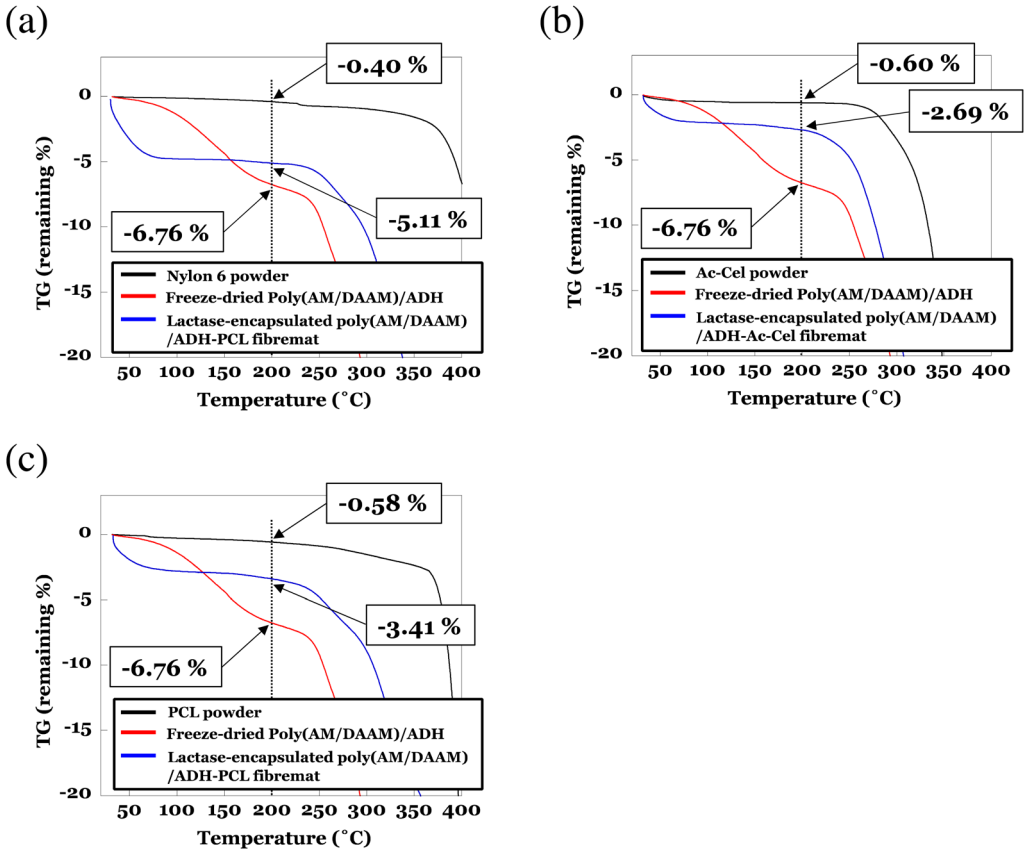

Fig. 9 Thermogravimetric (TG) analyses of lactase-encapsulated poly(AM/DAAM)/ADH core–shell fibremats fabricated with (a) nylon6, (b) AcCel, or (c) PCL shell layers. As references, TG data for freeze-dried poly(AM/DAAM)/ADH hydrogel gels (*i.e.*, core-nanofibre material) and nylon6, AcCel, and PCL powders (*i.e.*, shell-layer materials) are also presented in each graph. All samples were heated at 10 °C min^{-1} under N_2 gas constantly flowing at 200 mL min^{-1} to sample chamber and analysed using TG in range 30–550 °C. To determine amount of residual water as percentage of fibremat mass (wt%) in core–shell fibremats, TG data are magnified in range 30–400 °C. TG data over entire temperature range are shown in Fig. S1–3 (ESI).†

results are shown in Fig. S5 (ESI).† Clear endothermic peaks appeared at ~63 °C for the lactase-encapsulated poly(AM/DAAM)-nylon6 fibremat (Fig. S5(a)†). Because very little endothermic heat should be generated by the lactase encapsulated in the fibremat [*i.e.*, the 2–5 mg fibremat TG samples only contained 5–10 μg of encapsulated lactase; Fig. S5(d)†], the peak should originate from water evaporating from the fibremats. Furthermore, because the endothermic heat peaks of the nylon6 powder (at ~40 °C, corresponding to water evaporating from nylon6) were different from those of the fibremats (at ~63 °C), the heat peaks at ~63 °C correspond to water evaporating from the fibremat core-nanofibres. Nesrinne *et al.* reported DSC data for polyacrylamide and attributed the peaks at ~50 and ~90 °C to the water evaporation and glass transition of polyacrylamide, respectively.[34] Additionally, because these temperatures can be altered by including other monomer units in the polyacrylamide,[34] our interpretation of the heat peak at ~63 °C is reasonable. Furthermore, the heat peak for the core–shell fibremat fabricated with the AcCel shell appeared at a temperature like that for the AcCel powder (~45 °C). The peaks corresponding to water evaporating from the core nanofibres and AcCel (*i.e.*, shell material) almost overlapped, implying that very little water was inside the core nanofibres. Owing to the concomitant sharp PCL-T_m-derived endothermic heat peak at ~62 °C,[35] a detailed analysis of the water evaporating from the lactase-encapsulated poly(AM/DAAM)-PCL fibremat was difficult. However, the overlapping broad endothermic heat peaks from 20 to 100 °C also implied that residual water was inside the core nanofibres. More endothermic heat originated from the lactase-encapsulated poly(AM/DAAM)-nylon6 core-nanofibres than from the other core–shell fibremats, which also implies that the fibremats fabricated with nylon6 shell layers were the best among all the core–shell fibremats examined to date for encapsulating and functionalising lactase inside core nanofibres.

Characterisation of enzymatic activities and re-usability of encapsulated lactase

The enzymatic activities of the lactase encapsulated in the core–shell fibremats were evaluated using 2-nitrophenyl-β-1-galactopyranoside (ONPG; Mw = 301.3) as a dummy substrate[36] of the original, lactose (Mw = 342.3). Because the elimination of 2-nitrophenol by the hydrolysis of the ONPG β-1-glycosidic linkage produces a yellow solution in the basic pH range, the

Table 2 Enzymatic activities of lactase-encapsulated core–shell fibremats and free enzyme (control)

	Enzymatic activity (nmol min^{-1} mg^{-1})	Ratio to enzymatic activity of control (%)
Control (free enzyme)	3580 ± 160	—
Poly(AM/DAAM)/ADH-PCL fibremat[a]	3610 ± 90	101
Poly(AM/DAAM)/ADH-Nylon6 fibremat[a]	4080 ± 90	114
Poly(AM/DAAM)/ADH-AcCel fibremat[a]	1480 ± 50	41

[a] FITC-labelled lactase was used for evaluating enzymatic activities because it accurately quantified contents of lactase encapsulated in core–shell fibremats, which were estimated at 2.8, 1.0, and 3.1 μg mg^{-1} [FITC-labelled lactase (μg) fibremat (mg^{-1})] for poly(AM/DAAM)/ADH-nylon6, -PCL, and -AcCel fibremats, respectively.

progress of enzymatic reactions can be traced by measuring the changes in the absorbance at 415 nm (A_{415}). First, the lactase-encapsulated fibremats were stirred and equilibrated in a phosphate buffer (pH 7; 50 mM) at 37 °C. Then, the ONPG was added to a final concentration of 5.3 mM to initiate the enzymatic reaction. After 20 min, the fibremats were removed from the reaction solution. The supernatant pH was adjusted to 10 by adding aqueous Na_2CO_3 (500 mM), and the supernatant A_{415} was measured to determine the amount of the product formed, wherein 1 enzymatic activity unit was defined as the amount of the substrate that reacted with 1 mg of lactase in 1 min. Then, the enzymatic activity (in nmol min^{-1} mg^{-1}) of each fibremat (Table 2) was estimated from the linearly fitted amount of produced 2-nitrophenol plotted as functions of the lactase weight (Fig. 10). Compared to the free-enzyme activity, the enzymatic activities of the lactase-encapsulated fibremats fabricated using the nylon6, PCL, or AcCel shell layers were 114, 101, or 41%, respectively. Therefore, the nylon6 shell layer exhibited the best enzymatic activity (4080 ± 2 nmol $min^{-1}mg^{-1}$).

Interestingly, because of the locally increased enzyme concentration and local hydrophilicity within the restricted volume of the core nanofibres,[8] the enzymatic activity of the poly(AM/DAAM)/ADH-nylon6 core–shell fibremat was superior to that of the free enzyme. Meanwhile, the enzymatic activity of the poly(AM/DAAM)/ADH-AcCel core–shell fibremat (1480 ± 1 nmol min^{-1} mg^{-1}) was considerably lower than that of the free enzyme. Because the fibremats prepared using the different shell layers did not exhibit different low-Mw molecular permeabilities, the different enzymatic activities were likely attributable to the similar molecular structures of the repeating units of AcCel and ONPG. Because the AcCel neighbours the core nanofibre, the inter-molecular interactions between the AcCel repeating unit and encapsulated lactase could interfere with the ONPG binding to the lactase encapsulated in the core nanofibres, which is supported by the finding that encapsulating other enzymes such as lipase negligibly impacted the enzymatic hydrolysis of the ester substrate (data are not shown).[37] We believe that this phenomenon is a feature of the core–shell-fibremat-based enzyme immobilisation platform.

The re-usability of the lactase-encapsulated fibremats was further evaluated using the recovered fibremats for the next enzymatic reactions. Prior to re-use for the next reaction, the recovered fibremats were washed in water thrice and dried by sandwiching between paper towels. The enzymatic activities estimated after each re-use are shown as a percentage (%) of the initial enzymatic activity in Fig. 11. Even after being re-used 10 times, the fibremats fabricated using the PCL or nylon6 shells retained more than 95% of the initial enzymatic activity. In industrial enzyme immobilisation applications, the substrate re-usability is sometimes problematic, especially in aqueous solvents. In general, physisorption (*i.e.*, electrostatic adsorption) is preferred rather than covalent immobilisation, so that

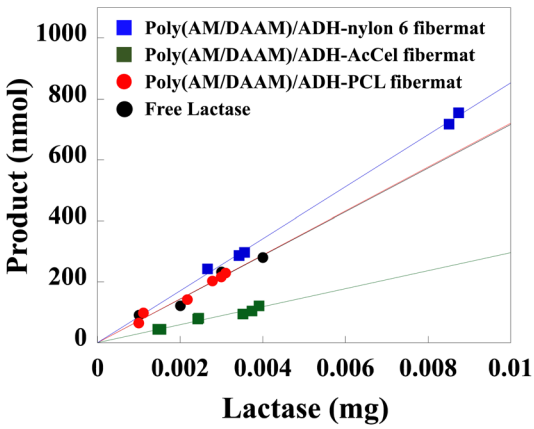

Fig. 10 Enzymatic activities estimated from produced 2-nitrophenol (nmol) plotted as functions of lactase weight (mg) encapsulated in core–shell fibremats or free lactase. Enzymatic reaction was performed for 20 min in 4 mL of phosphate buffer (pH 7; 50 mM) containing ONPG (5.3 mM).

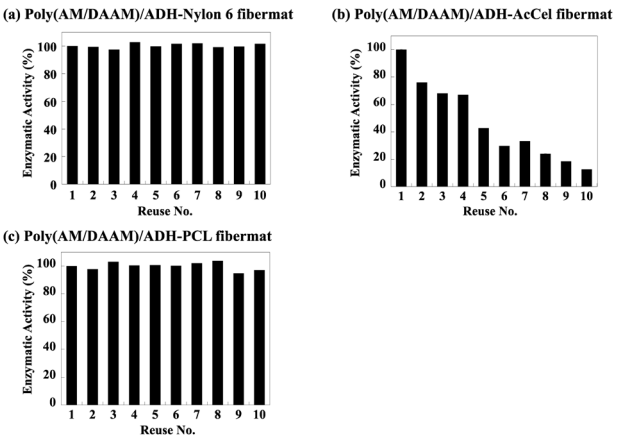

Fig. 11 Lactase enzymatic activities for poly(AM/DAAM)/ADH- (a) nylon6, (b) AcCel, and (c) PCL fibremats re-used 1–10 times expressed as percentages (%) of initial enzymatic activity.

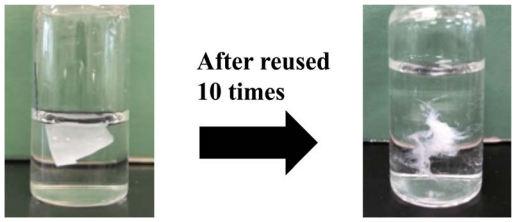

Fig. 12 Defibration of poly(AM/DAAM)/ADH-AcCel re-used 10 times.

the negative impacts on the enzymatic activity could be reduced through enzyme immobilisation.[38] However, in aqueous media, enzyme molecules immobilised by physisorption, are easily detached from immobilisation substrates. In this enzyme immobilisation platform, on the other hand, the enzyme molecules were stably held in the core–shell fibremat nanofibres, and the obtained enzymatic activity was comparable to or higher than the original one, meaning that this enzyme immobilisation platform is clearly superior to conventional ones.[6]

Meanwhile, owing to the low adhesion between the poly(AM/DAAM)/ADH-AcCel nanofibres, the obtained enzymatic activities considerably decreased with increasing number of substrate re-uses because the detached enzyme-encapsulated nanofibres defibrated from the entire fibremat. As shown in Fig. 12, the fibremat was clearly destroyed when the film was re-used 10 times, meaning that although the shell-layer material was negligibly affected by the enzymatic activity and substrate re-usability, the substrate exhibited inferior re-usability when the fibremat film morphology was destabilised.

Experimental

Materials

Unless stated otherwise, all the chemicals and reagents were commercially obtained and used without further purification. *Tris*(hydroxymethyl)aminomethane (Tris), *o*-nitrophenyl-β-D-galactopyranoside (ONPG),[36] acrylamide, 2,2,2-trifluoroethanol (TFE), 2,2′-azo*bis*[*N*-(2-carboxyethyl)-2-methylpropionamidine] tetrahydrate (VA-057), disodium phosphate (Na_2HPO_4), sodium dihydrogen phosphate (NaH_2PO_4), and fluorescein were purchased from Wako Pure Chemical Industries, Ltd (Japan). Diacetone acrylamide (DAAM) and adipic dihydrazide (ADH) were purchased from Tokyo Chemical Industry Co., Ltd (Japan). DAAM was re-crystallised several times from ethyl acetate to remove the inhibitor (mequinol) before use in the reversible addition-fragmentation chain transfer (RAFT) polymerisation.[28] Lactase,[25] nylon6 (Cat. No., 181110), and acetyl cellulose (AcCel; M_n = 30 000) were purchased from Sigma-Aldrich (USA). Poly(AM/DAAM) featuring AM and DAAM combined in a molar ratio of 4 : 1, was synthesised as described in our previous paper[17] by replacing the poly(AM/DAAM) with PAM-*co*-PDAAM. The FITC-labelled lysozyme was synthesised using the method described in a previous study.[1] The M_n and polydispersity index (PDI) of the poly(AM/DAAM) were calculated from the GPC profile calibrated using poly(ethylene glycol) (PEG) standards.

Construction of core–shell fibremats with/without encapsulated proteins or fluorescent molecules

ADH [0.5 molar equivalent with respect to the poly(AM/DAAM) DAAM unit] was added to a poly(AM/DAAM) solution [0.5 g dissolved in 2.5 mL of phosphate buffer (100 mM; pH 8)] and transferred to a Luer-Lok syringe (5 mL). To encapsulate proteins such as the FITC-labelled lactase, 1 wt% of the protein (with respect to the polymer mass) was added to the solution. To encapsulate fluorescent molecules such as fluorescein, 0.4 mmol of the fluorescent molecule was added to the solution. Concomitantly, either a 10 wt% nylon6 or 13 wt% AcCel solution dissolved in TFE was prepared and transferred to another Luer-Lok syringe (5 mL). Both syringes were then placed in different syringe pumps fitted with a linear actuator (KDS-100, KD Scientific, USA) and connected to a co-axial spinneret (MECC Co., Ltd, Japan) equipped with 27 G needle (Terumo Corp.) for passing the poly(AM/DAAM)/ADH) core solution through a polytetrafluoroethylene (PTFE) tube. The poly(AM/DAAM)/ADH, nylon6, or AcCel solutions were then electrospun (SD-02, MECC Co., Ltd, Japan) at linear extrusion velocities of 0.2, 1.0, or 1.2 mL h^{-1}, respectively, at a high voltage (20 kV). The obtained fibremat core and shell components were poly(AM/DAAM)ADH and either nylon6 or AcCel, respectively. The distance between the spinneret tip and electrically grounded collector (aluminium plate; 150 × 200 mm) was set to 160 or 190 mm for constructing the poly(AM/DAAM)/ADH-nylon6 or -AcCel fibremat, respectively.

Scanning electron microscopy (SEM)

The samples were coated with amorphous osmium by plasma chemical vapour deposition using an OPC60A vacuum evaporator (Filgen, Inc., Japan). The sample morphologies were examined using field-emission SEM (JSM-7800F, JEOL, Japan) operating at 3 kV acceleration. The fibremat nanofibre mean diameters and corresponding standard deviations were evaluated using the SEM images of 30 nanofibres and Image J software.

Transmission electron microscopy (TEM)

The TEM samples were prepared by directly collecting the electrospun core–shell nanofibres from the co-axial spinneret on a TEM grid comprising a formvar carbon film on a 100-mesh copper wire grid (50) [Okenshoji Co., Ltd, Japan]. To obtain adequate image contrast between the core and shell, sodium phosphotungstate was mixed at a final concentration of 0.04% (w/v) with the core precursor solution comprising poly(AM/DAAM) and ADH. The TEM images were acquired using a JEM-1400Plus instrument (JEOL, Japan) operating at 100 kV acceleration.

Attenuated total-reflectance Fourier-transform infrared (ATR-FTIR) spectroscopy

The ATR-FTIR spectra were acquired using an FT-IR-4000 spectrometer (JASCO, Japan) equipped with an ATR PRO450-S unit (JASCO, Japan). The free-induction-decay (FID) spectra

were scanned 200 times at 25 °C, accumulated, and Fourier-transformed to obtain the FTIR spectra at a resolution of 4 cm^{-1}.

Leakage/release of encapsulated fluorescein or FITC-labelled lysozyme upon fibremat immersion in buffer

The loaded fibremats (1 mg) were cut in square pieces (5 × 5 mm; 1 mg) and placed in a 24-well plate and immersed in 1.0 mL of phosphate buffer (pH 7; 50 mM) for defined periods (0–3 h) at 25 °C and gently orbitally shaken at 100 rpm. The fibremats were then removed from the buffer, and the F_{520} values of the remaining solutions were measured using a plate reader (SH-9000Lab, Hitachi, Japan). By comparison to the standard curve, the fluorophore release degree was determined during the assay period.

Fibremat tensile-strength measurements

To test the fibremat tensile strengths, the fibremats were cut into 20 mm-long × 5 mm-wide dumbbell-shaped pieces and set between the sensor tips of a testing machine (Autograph, AGS-G, Shimadzu, Japan) equipped with a 50 N-load cell, according to the Japanese Industrial Standard (JIS L 1015). The mechanical tests were performed over a 20 mm-long span at a cross-head velocity of 1 mm min^{-1} for $n = 5$ specimens.

Thermal analyses by thermogravimetry (TG), differential thermal analysis (DTA), and differential scanning calorimetry (DSC)

TG and DTA measurements were performed using a Thermogravimeter–Differential Thermal Analyser (TG/DTA 7300, Hitachi High-Tech Science Corporation, Japan) from 30 to 550 °C. The samples were heated at 10 °C min^{-1} under N_2 gas constantly flowing at 200 mL min^{-1} to the sample chamber. DSC measurements were performed using a differential scanning calorimeter (DSC7000X, Hitachi High-Tech Science Corporation, Japan) from 0 to 200 °C. The samples were heated at 5 °C min^{-1} under N_2 gas constant flowing at 30 mL min^{-1}. For the TG, DTA, and DSC measurements, circular (⌀4 mm) fibremat samples (2–5 mg) were cut and filled in aluminium sample pans (⌀5.2 mm).

Preparation of FITC-labelled lactase[30]

To determine precisely the amount of lactase encapsulated in the prepared fibremats, fluorescently labelled lactase was used. The FITC-labelled lactase was prepared as follows: First, lactase (800 mg) was dissolved in a phosphate buffer (pH 8; 60 mM). Then, FITC (7.1 mg; 18.2 μmol) was added to this mixture, which was further stirred at 4 °C for 18 h. This mixture was dialysed (Visking tubing; cut-off Mw: 12–14 kDa; Japan Medical Science, Inc., Japan) against deionised H_2O, concentrated, and applied to gel filtration chromatography [Sephadex® G-50; phosphate buffer (pH 7; 50 mM) eluent] to purify the FITC-labelled lactase. The purity was confirmed using sodium dodecyl sulphate polyacrylamide gel electrophoresis (SDS–PAGE) analysis.

Evaluation of enzymatic activities for enzyme-encapsulating core–shell fibremats

The core–shell fibremats encapsulating 1–3 mg of the FITC-labelled lactase were immersed in 0.5 mL of a phosphate buffer (pH 7; 50 mM) and stabilised at 37 °C using a thermostatic incubator. The FITC-labelled lactase contents were 2.8, 1.0, and 3.1 μg mg^{-1} [FITC-labelled lactase (μg) fibremat (mg^{-1})] in the poly(AM/DAAM)/ADH-nylon6, -PCL, and -AcCel fibremats, respectively. Then, 3.5 mL of ONPG (6 mM) dissolved in the phosphate buffer (pH 7; 50 mM) was added so that the final ONPG concentration was 5.25 mM, and the enzymatic reaction mixture was gently stirred. After incubation for 20 min at 37 °C, the enzymatic reaction was terminated by removing the fibremats from the reaction solution. Then, 1 mL of aqueous $NaCO_3$ (500 mM) was added to the mixture, and A_{415} was measured to determine the product amount. For the controls, phosphate buffer solutions (pH 7; 50 mM) containing 1, 2, 3, or 4 μg of FITC-lactase and ONPG (5.25 mM) were used to determine the enzymatic activities. Additionally, the enzymatic activities were determined for the fibremats re-used multiple times by recovering the fibremats used in the previous reaction for the next one. Prior to use in the next reaction, the recovered fibremats were washed by immersion in deionised H_2O (4 mL) thrice (×3) for 30 min and then dried by sandwiching between paper towels.

Conclusions

To evaluate the versatility of the core–shell fibremats comprising poly(AM/DAAM)/ADH core-nanofibres and hydrophobic polymer shell layers as an enzyme immobilisation platform, we examined the impacts of the shell-layer material of the enzyme-encapsulated core–shell fibremat on the enzymatic activity, substrate re-usability, and operativity. The lactase-encapsulated poly(AM/DAAM)/ADH·nylon6 and ·AcCel fibremats were both constructed like the poly(AM/DAAM)/ADH-PCL one. All the core–shell fibremats exhibited efficient low-Mw substrate permeability and stably held the enzyme molecule without leakage. The good low-Mw molecular permeability regardless of the shell-layer material might be attributed to the formation of the inter-connected nanostructures in the shell layer, as implied by the wrinkles on the fibremat nanofibre surfaces. Depending on the mechanical properties of the original shell materials, those of the core–shell fibremats can be controlled by choosing the shell-layer material, which sometimes considerably impacts both the fibremat enzymatic activity and re-usability. Because the shell-material repeating unit and enzyme substrate exhibited similar molecular structures, the poly(AM/DAAM)/ADH-AcCel exhibited a substantially decreased enzymatic activity. Because the film morphology destabilised, the poly(AM/DAAM)/ADH-AcCel fibremat could be re-used fewer times than the -nylon6 and -PCL ones. These results indicate the usefulness of the proposed core–shell-fibremat-based enzyme-immobilisation platform comprising a hydrophobic polymer shell and core nanofibres prepared using a pair of post-cross-linkable hydrophilic polymers and bifunctional cross-linkers such as poly(AM/DAAM) and ADH.

Author contributions

T. Mizuno conceived the project. T. Ishiguro and T. Mizuno designed the experiments. T. Ishiguro, A. Obata, K. Nagata, and T. Kasuga performed the experiments and data analysis. T. Mizuno wrote the manuscript. All the authors edited and approved the finalised manuscript.

Conflicts of interest

There are no conflicts to declare.

Acknowledgements

We appreciate Dr Shinichi Matsuoka (Graduate School of Engineering, Nagoya Institute of Technology) helping GPC analysis of poly(AM/DAAM). This work was supported by the JST A-STEP (Grant no. JPMJTM20EH, Adaptable and Seamless Technology Transfer Program through Target-driven R&D) and the Toshiaki Ogasawara Memorial Foundation.

Notes and references

1 Y. Tanikawa, Y. Ido, R. Ando, A. Obata, K. Nagata, T. Kasuga and T. Mizuno, *Bull. Chem. Soc. Jpn.*, 2020, **93**, 1155–1163.
2 A. Basso and S. Serban, *Methods Mol. Biol.*, 2020, **2100**, 27–63.
3 M. B. Ansorge-Schumacher and O. Thum, *Chem. Soc. Rev.*, 2013, **42**, 6475–6490.
4 V. P. Torchilin, *Adv. Drug Delivery Rev.*, 1988, **1**, 270.
5 J. Zdarta, K. Jankowska, K. Bachosz, O. Degorska, K. Kazmierczak, L. N. Nguyen, L. D. Nghiem and T. Jesionowski, *Curr. Pollut. Rep.*, 2021, **7**, 167–179.
6 E. D. Yushkova, E. A. Nazarova, A. V. Matyuhina, A. O. Noskova, D. O. Shavronskaya, V. V. Vinogradov, N. N. Skvortsova and E. F. Krivoshapkina, *J. Agric. Food Chem.*, 2019, **67**, 11553–11567.
7 H. C. Chang, A. Ueno, H. Yamada, T. Matsue and I. Uchida, *Analyst*, 1991, **116**, 793–796.
8 J. G. Yifei Zhang and L. Zheng, *ACS Catal.*, 2015, **5**, 4503–4513.
9 S. Badieyan, Q. Wang, X. Zou, Y. Li, M. Herron, N. L. Abbott, Z. Chen and E. N. Marsh, *J. Am. Chem. Soc.*, 2017, **139**, 2872–2875.
10 G. Ferrand-Drake Del Castillo, M. Koenig, M. Muller, K. J. Eichhorn, M. Stamm, P. Uhlmann and A. Dahlin, *Langmuir*, 2019, **35**, 3479–3489.
11 V. L. Sirisha, A. Jain and A. Jain, *Adv. Food Nutr. Res.*, 2016, **79**, 179–211.
12 M. R. Khan, *Bull. Natl. Res. Cent.*, 2021, **45**, 207.
13 A. S. Amirhossein Ahmadian, N. Aliahmad and M. Agarwal, *Textiles*, 2021, **1**, 206–226.
14 R. S. Khan, A. H. Rather, T. U. Wani, S. U. Rather, T. Amna, M. S. Hassan and F. A. Sheikh, *Biotechnol. Bioeng.*, 2022, DOI: 10.1002/bit.28246.
15 A. Obata, S. Ito, N. Iwanaga, T. Mizuno, J. R. Jones and T. Kasuga, *RSC Adv.*, 2014, **4**, 52491–52499.
16 S. Koeda, K. Ichiki, N. Iwanaga, K. Mizuno, M. Shibata, A. Obata, T. Kasuga and T. Mizuno, *Langmuir*, 2016, **32**, 221–229.
17 Y. Ido, A. L. B. Macon, M. Iguchi, Y. Ozeki, S. Koeda, A. Obata, T. Kasuga and T. Mizuno, *Polymer*, 2017, **132**, 342–352.
18 M. M. Hausladen, B. Zhao, M. S. Kubala, L. F. Francis, T. M. Kowalewski and C. J. Ellison, *Proc. Natl. Acad. Sci. U. S. A.*, 2022, **119**, e2201776119.
19 G. K. Gueorguiev, S. Stafstrom and L. Hultman, *Chem. Phys. Lett.*, 2008, **458**, 170–174.
20 A. M. Evans, M. J. Strauss, A. R. Corcos, Z. Hirani, W. Ji, L. S. Hamachi, X. Aguilar-Enriquez, A. D. Chavez, B. J. Smith and W. R. Dichtel, *Chem. Rev.*, 2022, **122**, 442–564.
21 M. Askari, M. Afzali Naniz, M. Kouhi, A. Saberi, A. Zolfagharian and M. Bodaghi, *Biomater. Sci.*, 2021, **9**, 535–573.
22 E. Mueller, I. Poulin, W. J. Bodnaryk and T. Hoare, *Biomacromolecules*, 2022, **23**, 619–640.
23 I. D. S. Christos Koukiotis, *Prog. Org. Coat.*, 2010, **69**, 504–509.
24 Z. C. Sun, E. Zussman, A. L. Yarin, J. H. Wendorff and A. Greiner, *Adv. Mater.*, 2003, **15**, 1929.
25 M. M. Maksimainen, A. Lampio, M. Mertanen, O. Turunen and J. Rouvinen, *Int. J. Biol. Macromol.*, 2013, **60**, 109–115.
26 M. Nouri-Felekori, N. Nezafati, M. Moraveji, S. Hesaraki and T. Ramezani, *Int. J. Biol. Macromol.*, 2021, **183**, 2030–2043.
27 D. M. Patterson, L. A. Nazarova and J. A. Prescher, *ACS Chem. Biol.*, 2014, **9**, 592–605.
28 C. L. McCormick and A. B. Lowe, *Acc. Chem. Res.*, 2004, **37**, 312–325.
29 P. Peets, I. Leito, J. Pelt and S. Vahur, *Spectrochim Acta A*, 2017, **173**, 175–181.
30 Y. Z. Zhao, X. Q. Tian, M. Zhang, L. Cai, A. Ru, X. T. Shen, X. Jiang, R. R. Jin, L. Zheng, K. Hawkins, S. Charkrabarti, X. K. Li, Q. Lin, W. Z. Yu, S. Ge, C. T. Lu and H. L. Wong, *J. Controlled Release*, 2014, **186**, 22–31.
31 Z. H. Lu, B. W. Zhang, H. Gong and J. S. Li, *Polymer*, 2021, 226.
32 H. Yabu, *Sci. Technol. Adv. Mater.*, 2018, **19**, 802–822.
33 A. Z. S. Galal Ibrahim, A. E. Hamada and M. Mohamed Sayah, *Am. j. polym. sci.*, 2019, **5**, 55–62.
34 S. Nesrinne and A. Djamel, *Arabian J. Chem.*, 2017, **10**, 539–547.
35 S. Jana, M. Leung, J. Chang and M. Zhang, *Biofabrication*, 2014, **6**, 035012.
36 X. Zhang, H. Li, C. J. Li, T. Ma, G. Li and Y. H. Liu, *BMC Microbiol.*, 2013, **13**, 237.
37 T. Mizuno and T. Ishiguro, to be published in elsewhere.
38 Q. Y. M. E. Hassan and Z. Xiao, *Bull. Natl. Res. Cent.*, 2019, **43**, 102.